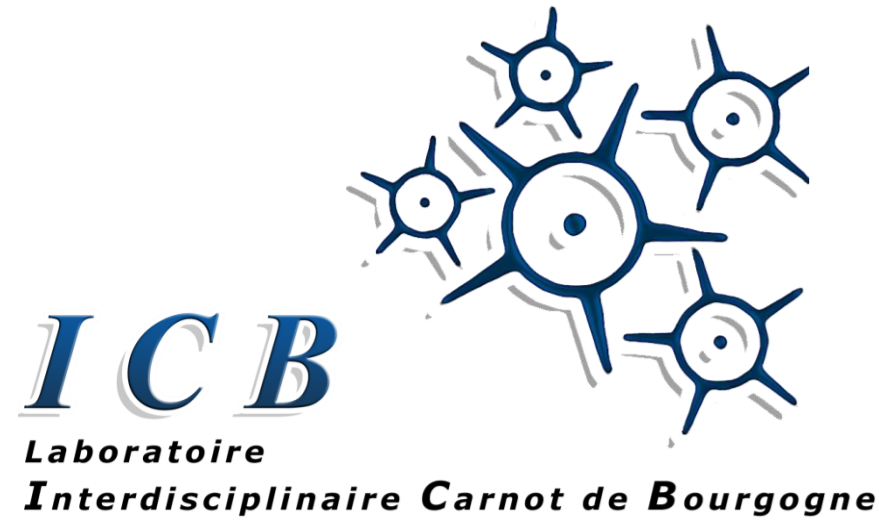


# Gain sideband splitting in dispersion oscillating fibers



Christophe FINOT<sup>1</sup> and Stefan WABNITZ<sup>2</sup>

1. Laboratoire Interdisciplinaire Carnot de Bourgogne, UMR 6303 CNRS-Université de Bourgogne, 9 avenue. A. Savary, BP 47 870, 21078 DIJON Cedex

2. Dipartimento di Ingegneria dell'Informazione, Università degli Studi di Brescia via Branze 38, 25123, Brescia, Italy

[christophe.finot@u-bourgogne.fr](mailto:christophe.finot@u-bourgogne.fr)



## Introduction

Modulation instability (MI) has been widely investigated in various fields of physics, e.g., plasma, hydrodynamics and optics. MI leads to the emergence and amplification of gain sidebands in the spectrum of an initially intense continuous wave. MI has been demonstrated in fibers with anomalous group-velocity dispersion (GVD), and in normal dispersion fibers with fourth order dispersion, birefringence or multimode coupling. More recently, renewed experimental and theoretical interest in the MI process has been stimulated by using fibers with a longitudinal and periodic modulation of the GVD. Indeed, thanks to parametric resonance induced by the periodic variation of GVD, scalar MI sidebands can emerge even in the normal average GVD regime of a dispersion-oscillating fiber (DOF). Recent experiments confirmed resonant MI in microstructure DOF around 1  $\mu\text{m}$ , and in non-microstructure, highly nonlinear DOF at telecom wavelengths.

So far, the role of the amplitude of GVD oscillations has been largely overlooked. In this contribution, we present a systematic study of the various sidebands which are numerically observed at the output of a DOF as the amplitude of the dispersion variations grows larger. We unveil the emergence of new sidebands as well as their splitting in sub-sidebands.

## Situation under investigation

Periodic and longitudinal evolution of the second order dispersion :

$$\beta_2(z) = \beta_{2av} + \beta_{2amp} \sin(2\pi z / \Lambda)$$

$\beta_{2av}$  the average second order dispersion  
 $\beta_{2amp}$  the amplitude of the dispersion fluctuation  
 $\Lambda$  the spatial period of the dispersion fluctuation

Evolution of the light  $\psi$  during the propagation is modeled by the Nonlinear Schrödinger Equation:

$$i \frac{\partial \psi}{\partial z} - \frac{\beta_2(z)}{2} \frac{\partial^2 \psi}{\partial t^2} + \gamma |\psi|^2 \psi + i \frac{\alpha}{2} \psi = 0$$

$\gamma$  nonlinear Kerr coefficient  
 $\beta_2(z), \alpha$  dispersion fluctuation, linear loss (gain) coefficient  
 $t, z$  temporal coordinate and propagation distance

Central frequency  $\Omega_p$  and gain  $G_p$  of the  $p^{\text{th}}$  gain QPM sideband (QPM: Quasi-Phase Matched) :

$$\Omega_p = \pm \sqrt{\frac{2\pi p / \Lambda - 2\gamma P}{\beta_{2av}}} \quad \text{and} \quad G_p = \exp \left[ 2\gamma P L \left| J_p \left( \frac{\beta_{2amp} \Omega_p^2}{2\pi / \Lambda} \right) \right|^2 \right]$$

Parameters under investigation:

We consider here a 12 km fiber with  $\gamma = 2 \text{ W}^{-1}\text{km}^{-1}$ ,  $\Lambda = 1 \text{ km}$  and  $\beta_{2av} = -0.5 \text{ ps/km/nm}$  pumped by a cw with an average power of 0.75 W.

## Influence of the amplitude of dispersion fluctuation

The influence of  $\beta_{2amp}$  is explored by varying this parameter between 0.5 and 7 ps/km/nm.  $\alpha=0$ .

Different behaviors can be observed according to  $\beta_{2amp}$  :

- standard QPM sidebands (Fig 1A);
- cancellation of QPM sidebands & emergence of cascaded four wave mixing sidebands (Fig 1B)
- QPM sideband splitting (Fig 1C).

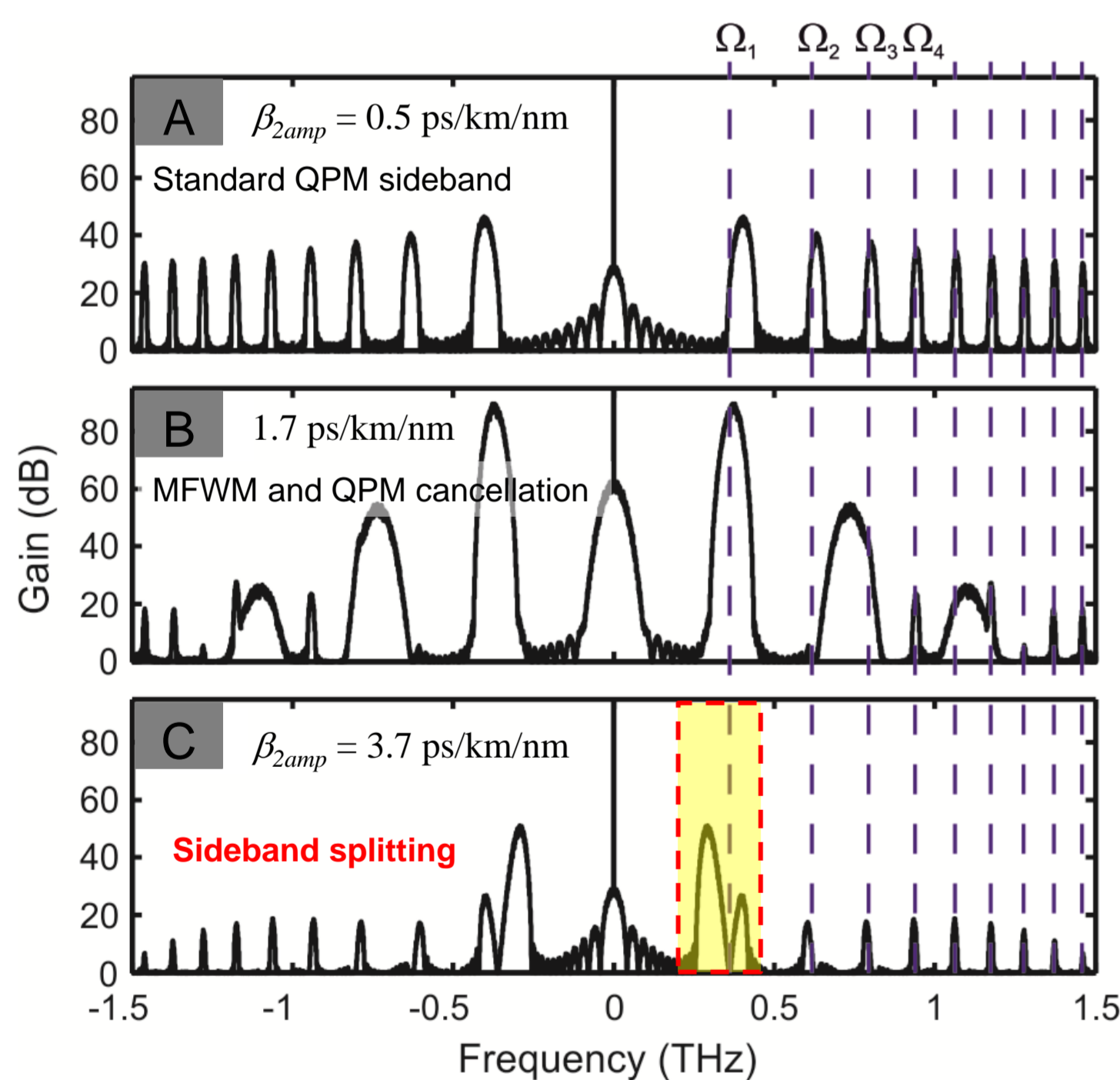


Figure 1 : Output spectrum for different values of the amplitude of dispersion fluctuations

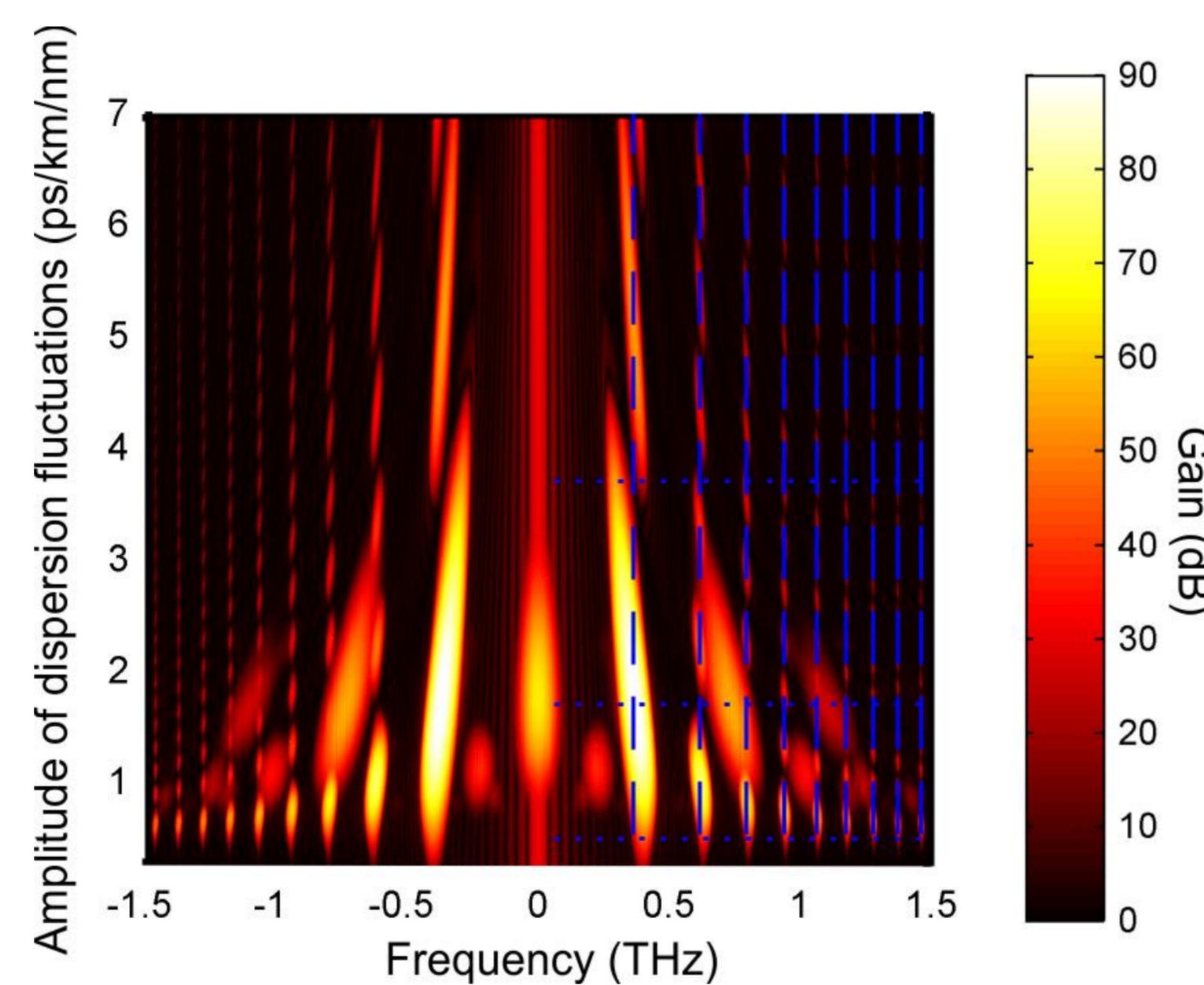


Figure 2 : Evolution of the output MI spectrum according to the level of dispersion fluctuation

The observation of the splitting does not violate the existing analytical laws.

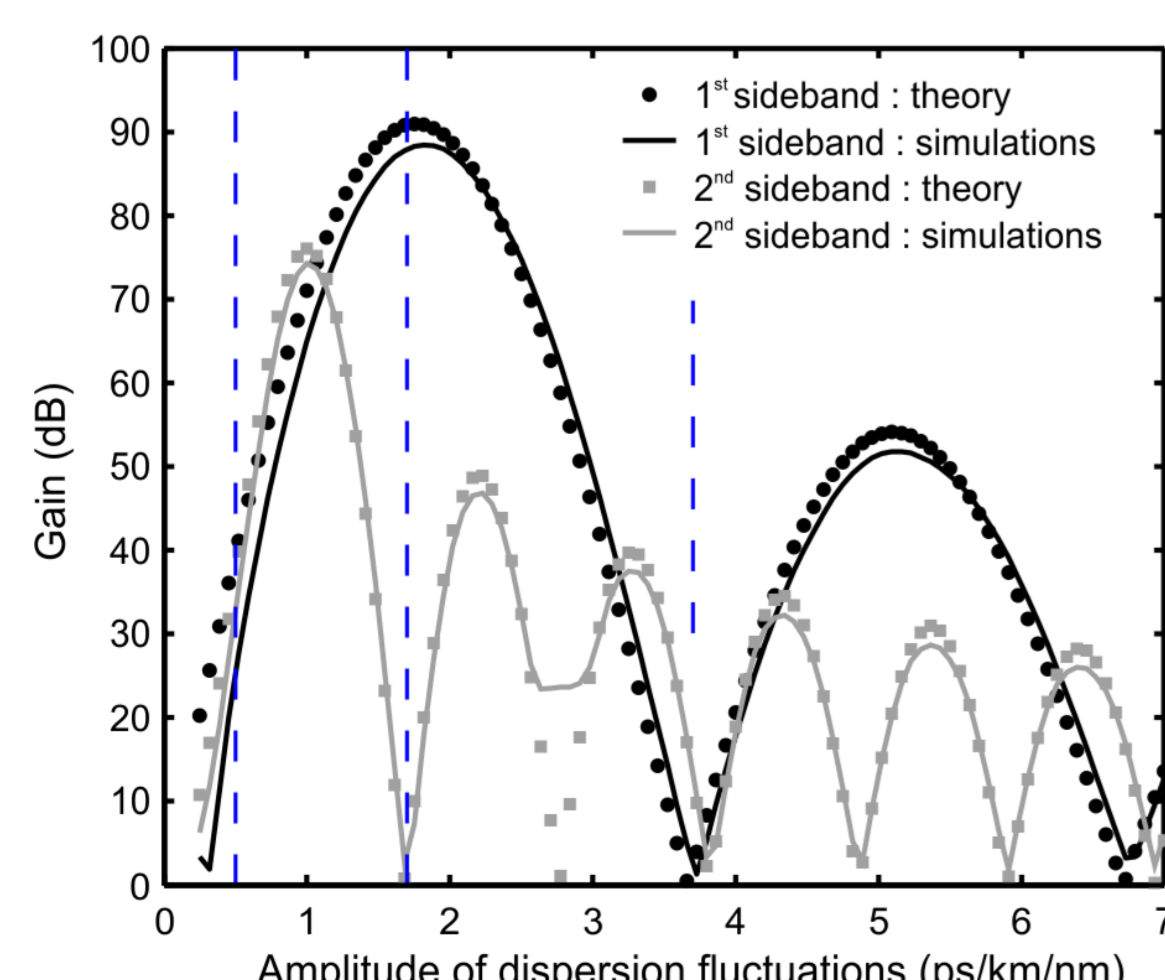


Figure 3 : Evolution with  $\beta_{2amp}$  of the gain at the frequencies  $\Omega_1$  and  $\Omega_2$  (black and grey colors respectively). Results obtained from numerical simulations (solid lines) are compared with analytical predictions  $G_1$  and  $G_2$  (circles and squares). Positions of the three cases reported in Fig. 1 are marked with dashed vertical lines.

The structure of the first QPM sideband can be qualitatively understood by an extension of  $G_1$  that was originally aimed at describing the gain at the QPM frequency  $\Omega_1$  only (see Fig. 5 & 6) :

$$G(\omega) = \exp \left[ 2\gamma P L \left| J_1 \left( \frac{\beta_{2amp} \omega^2}{2\pi / \Lambda} \right) \right|^2 \right]$$

## Floquet stability analysis

A quantitative analysis can be achieved using Floquet stability analysis

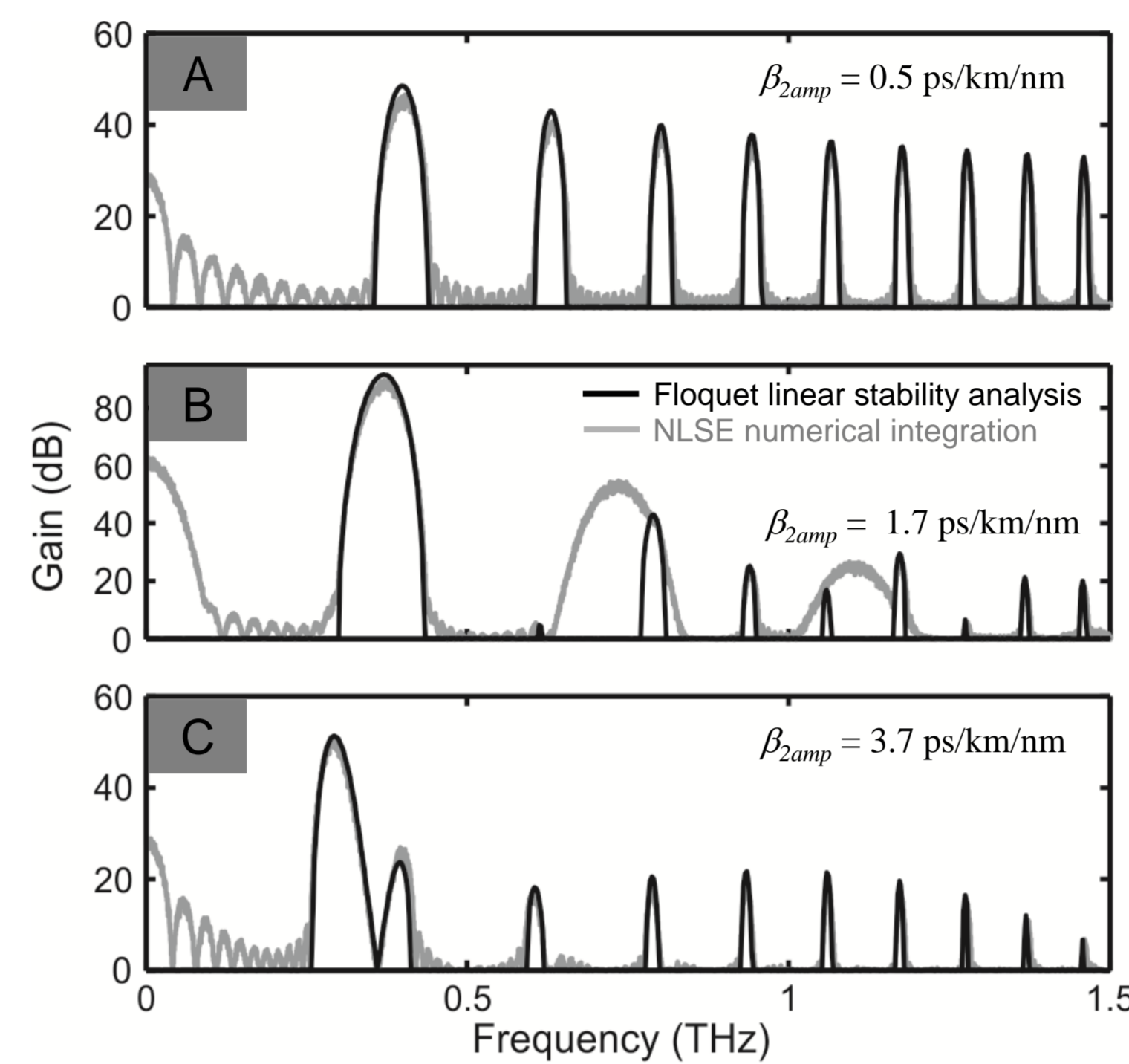


Figure 4 : Anti-Stokes sideband spectrum as Fig. 1. The results from the Floquet linear stability analysis are compared with the results of the numerical integration of NLS.

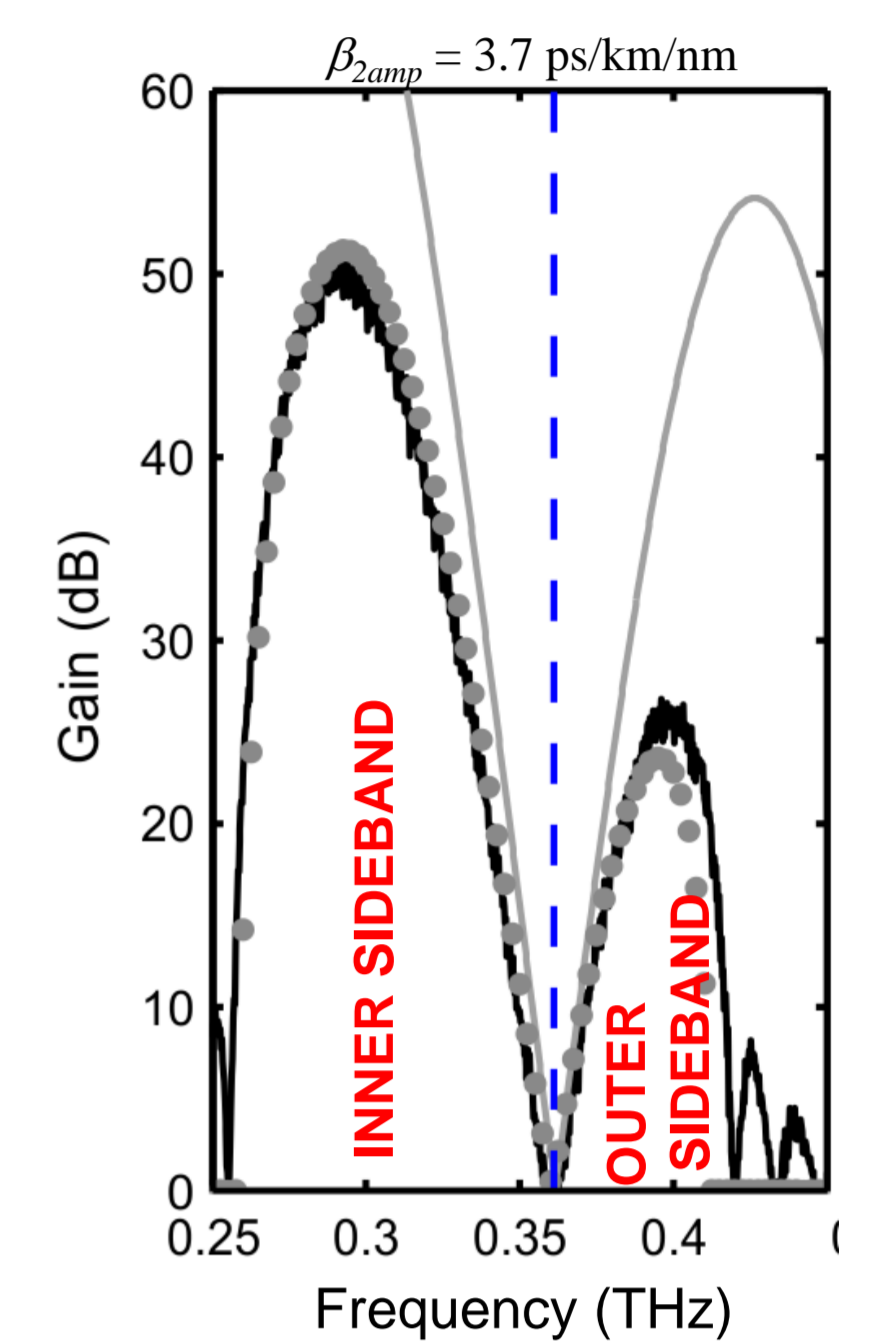


Figure 6 : Output spectrum after 12 kilometers of propagation obtained from numerical simulations (black line), from analytical equation  $G(\Omega)$  (grey line) and from the Floquet linear stability analysis (grey circles)

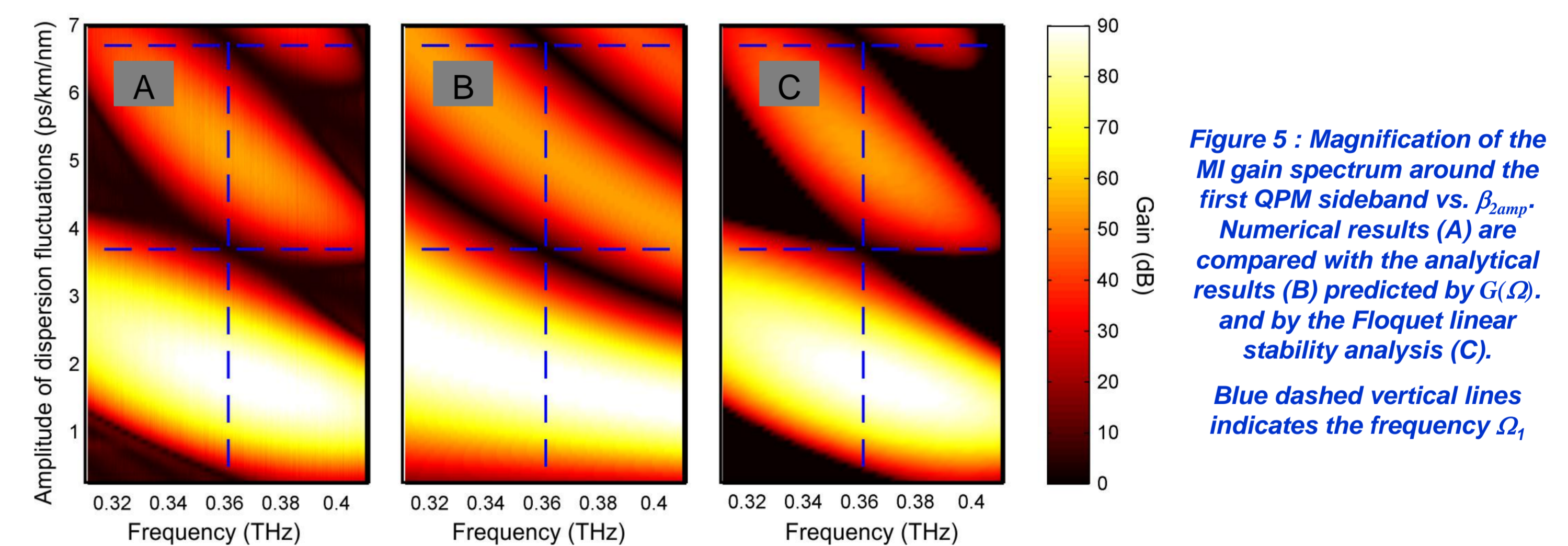


Figure 5 : Magnification of the MI gain spectrum around the first QPM sideband vs.  $\beta_{2amp}$ . Numerical results (A) are compared with the analytical results (B) predicted by  $G(\Omega)$ , and by the Floquet linear stability analysis (C). Blue dashed vertical lines indicates the frequency  $\Omega$ .

## Influence of distributed loss/gain

The presence of loss or gain strongly influences the shape of the output MI spectrum.

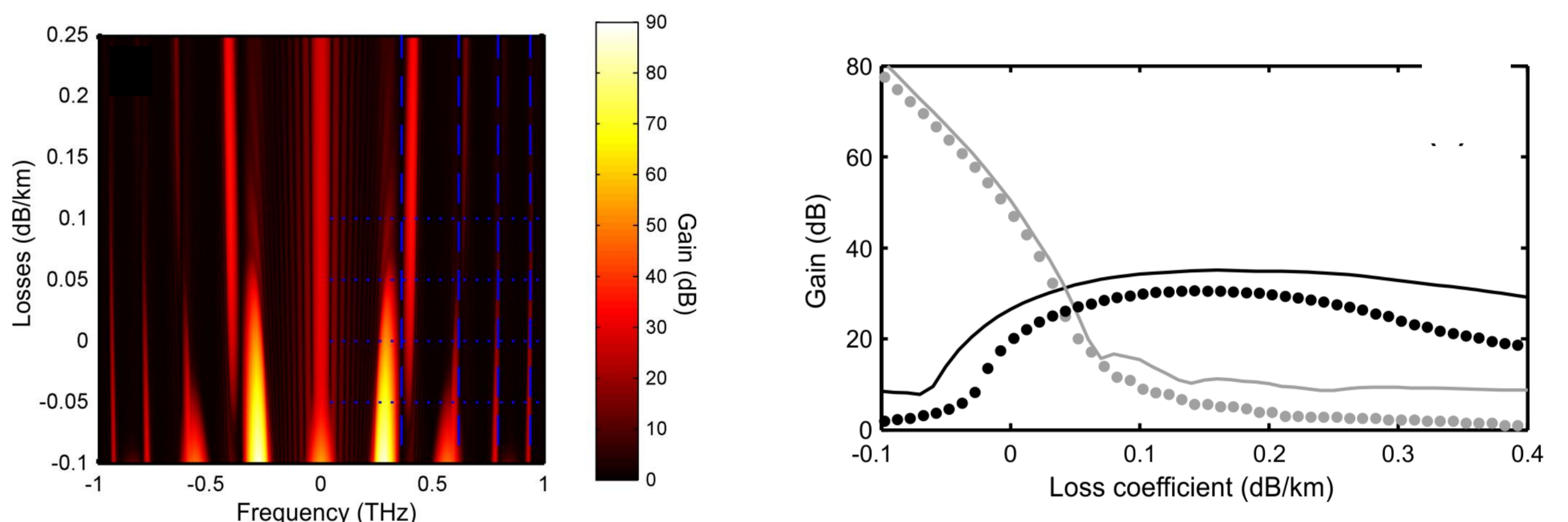


Figure 7 : Evolution of the output spectrum after 12 kilometers of propagation according to the level of linear losses/gain.

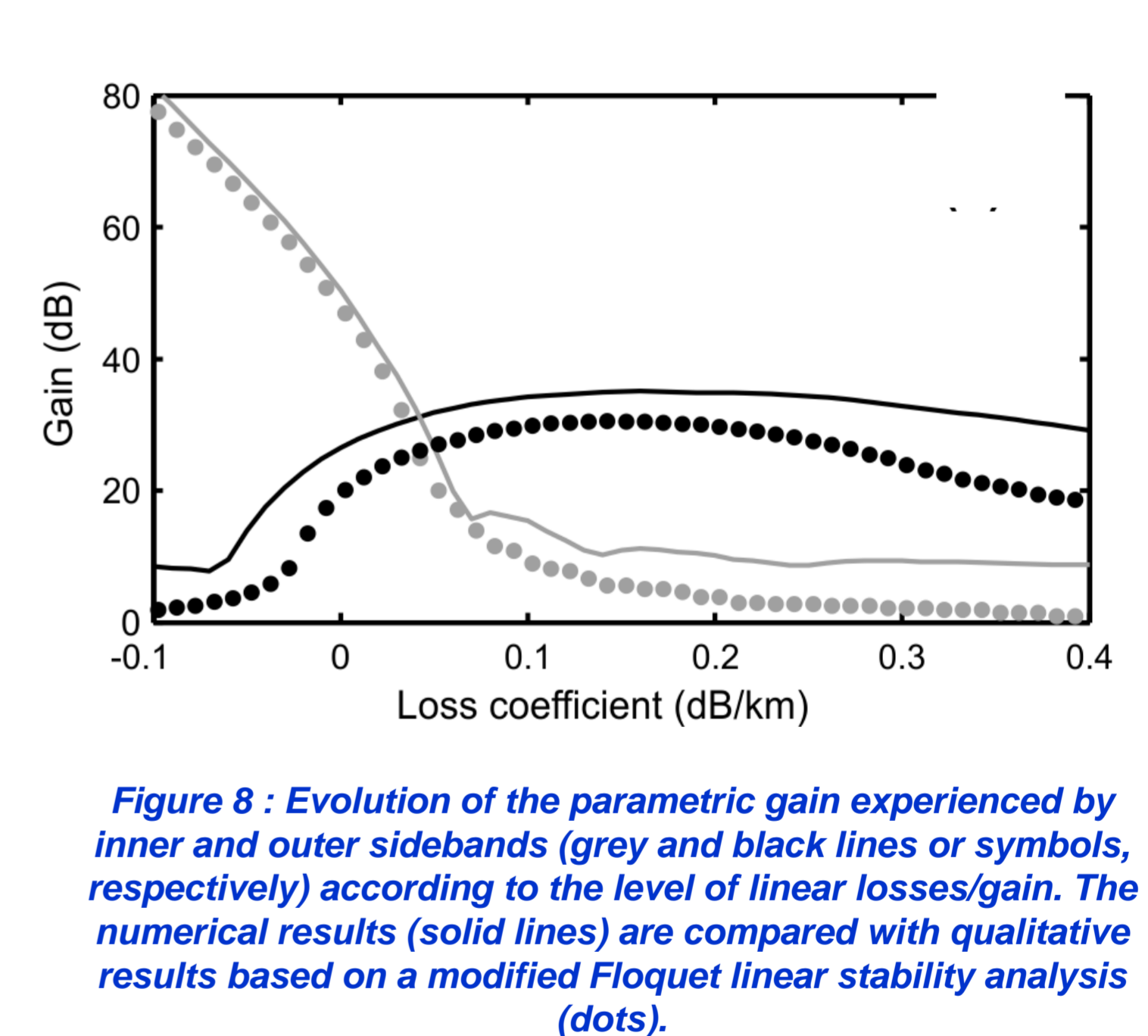


Figure 8 : Evolution of the parametric gain experienced by inner and outer sidebands (grey and black lines or symbols, respectively) according to the level of linear losses/gain. The numerical results (solid lines) are compared with qualitative results based on a modified Floquet linear stability analysis (dots).

Gain increases the level of the inner sideband, whereas loss reduces the inner sideband.

## Conclusion

We predicted the splitting of QPM-MI sidebands into two sub-sidebands in a DOF with large-amplitude dispersion oscillations. The existence of these two sidebands does not violate existing analytical predictions, and a link can be made with the parameters leading to an expected vanishing gain at the central resonant sideband frequency. The two sub-sidebands that emerge in the vicinity of the central QPM frequency can be qualitatively well reproduced by extending the analytical discrete resonant gain spectrum into a continuum of frequencies. A Floquet linear stability analysis provides an efficient tool to reproduce the structure of the sideband as well as the effects of loss/gain.

## Acknowledgement :

We thank Julien Fatome, Stéphane Pitois, Fang Feng, Yanne Chembo, Kamal Hammani and Alexej Sysoliatin for stimulating discussions. We acknowledge the financial support of the Conseil Régional de Bourgogne (Pari Photcom), the funding of the Labex ACTION program (ANR-11-LABX-01-01), and the Italian Ministry of University and Research (grant no. 2012BFNWZ2).

M. Droques, A. Kudlinski, G. Bouwmans, G. Martinelli, and A. Mussot, "Dynamics of the modulation instability spectrum in optical fibers with oscillating dispersion," Phys. Rev. A **87**, 013813 (2013).  
 N. J. Smith and N. J. Doran, "Modulation instabilities in fibers with periodic dispersion management," Opt. Lett. **21**, 570 (1996).  
 C. Finot, J. Fatome, A. Sysoliatin, A. Kosolapov, and S. Wabnitz, "Competing four-wave mixing processes in dispersion oscillating telecom fiber," Opt. Lett. **38**, 5361-5364 (2013).